Feature Article

JCBFM

Journal of Cerebral Blood Flow & Metabolism
2024, Vol. 44(2) 155–168

DOI: 10.1177/0271678X231201241
journals.sagepub.com/home/jcbfm
Sage

Whisker-evoked neurovascular coupling is preserved during hypoglycemia in mouse cortical arterioles and capillaries

Amy R Nippert*, Pei-Pei Chiang* and Eric A Newman

Abstract

Hypoglycemia is a serious complication of insulin treatment of diabetes that can lead to coma and death. Neurovascular coupling, which mediates increased local blood flow in response to neuronal activity, increases glucose availability to active neurons. This mechanism could be essential for neuronal health during hypoglycemia, when total glucose supplies are low. Previous studies suggest, however, that neurovascular coupling (a transient blood flow increase in response to an increase in neuronal activity) may be reduced during hypoglycemia. Such a reduction in blood flow increase would exacerbate the effects of hypoglycemia, depriving active neurons of glucose. We have reexamined the effects of hypoglycemia on neurovascular coupling by simultaneously monitoring neuronal and vascular responses to whisker stimulation in the awake mouse somatosensory cortex. We find that neurovascular coupling at both penetrating arterioles and at 2nd order capillaries did not change significantly during insulin-induced hypoglycemia compared to euglycemia. In addition, we show that the basal diameter of both arterioles and capillaries increases during hypoglycemia (10.3 and 9.7% increases, respectively). Our results demonstrate that both neurovascular coupling and basal increases in vessel diameter are active mechanisms which help to maintain an adequate supply of glucose to the brain during hypoglycemia.

Keywords

Neurovascular coupling, hypoglycemia, functional hyperemia, arterioles, capillaries

Received 13 February 2023; Revised 12 July 2023; Accepted 15 August 2023

Introduction

The brain has a high metabolic rate and requires a large, continuous supply of glucose and oxygen to function properly.[1] Functional hyperemia, the homeostatic response which results in increases in local blood flow evoked by neuronal activity, is one of several essential processes that ensure that the brain receives adequate glucose and oxygen under varying physiological conditions.[2] Functional hyperemia is mediated by neurovascular coupling, the signaling mechanism linking increased neuronal activity to dilation of nearby blood vessels.[2,3] The response is typically quantified as the ratio of the transient increase in local blood flow or transient vessel dilation to the increase in neuronal activity evoked by a sensory or electrical stimulus.

The supply of glucose to the brain is critical in diabetic patients, who can experience periods of hypoglycemia triggered by insulin administration.[4] In severe cases, hypoglycemia can lead to cognitive impairment,[5] coma, and death.[6] Neurovascular coupling, as the mechanism that maintains an adequate glucose supply to active neurons, is crucial under these hypoglycemic conditions. However, the effect of hypoglycemia on neurovascular coupling is not well characterized. A significant obstacle to accurately assessing neurovascular coupling is that both neuronal and vascular responses must be monitored simultaneously in order to quantify the response. If the hemodynamic response to a stimulus is reduced during hypoglycemia, for instance, the reduction could be due to a decrease in the magnitude of neurovascular coupling. However, it could also arise if there is a hypoglycemia-induced decrease in stimulus-evoked neuronal activity.

Department of Neuroscience, University of Minnesota, Minneapolis, Minnesota, USA

*These authors contributed equally to this work.

Corresponding author:
Eric A Newman, 321 Church St. SE, Minneapolis, MN 55455, USA.
Email: ean@umn.edu

To our knowledge, no previous studies have directly assessed whether neurovascular coupling is maintained, enhanced, or reduced during hypoglycemia. However, several studies have examined functional magnetic resonance imaging (fMRI) signals in response to visual,[7–9] or auditory[9] stimuli or motor action[10] in humans. These studies found that insulin-induced hypoglycemia (45–60 mg glucose/dL) reduced the fMRI response by 28 to 40%. Another study[11] found that the fMRI response to median nerve stimulation in the rat was reduced by 43% during hypoglycemia. If one assumes that the fMRI signal is proportional to the local cerebral blood flow (CBF) increase, the results suggest that hypoglycemia is accompanied by a decrease in neurovascular coupling. However, these studies did not measure the effect of hypoglycemia on stimulus-evoked neuronal responses. In contrast to the above studies, an investigation measuring regional CBF in humans with positron emission tomography[12] found no change in the CBF response to tactile stimulation during hypoglycemia.

In order to directly assess the effect of hypoglycemia on neurovascular coupling, we simultaneously measured neuronal and vascular responses to whisker stimulation in the whisker barrel cortex in awake, behaving mice. We hypothesized that neurovascular coupling would be reduced during hypoglycemia. Contrary to our expectations, we found that the magnitude of neurovascular coupling was not altered during hypoglycemia. In addition, we found that the basal diameter of both arterioles and capillaries increases during hypoglycemia.

Material and methods

Ethics statement

All experimental procedures were approved by and adhered to the guidelines of the Institutional Animal Care and Use Committee of the University of Minnesota, which is governed by the "Guide for the Care and Use of Laboratory Animals, 8th edition" of the National Research Council of the National Academies, USA (2011) as well as by the "Animal Care and Use in Research" guidelines of the National Institutes of Health, USA (2021). All experimental procedures adhered to the ARRIVE guidelines.

Animals

Experiments were performed on 10 to 18 week old male and female *Thy1*-GCaMP6s transgenic mice on a C57BL/6 background (RRID:IMSR_JAX:025776).

Surgery

Surgical methods have been described previously.[13] Prior to surgery, mice were treated with dexamethosane (2 mg/kg, American Pharmaceutical Partners, s.c.) to reduce the cortical stress response and prevent cerebral edema. In addition, the analgesic SR-Buprenex (1 mg/kg, Zoopharm, s.c.) and the antibiotic Cefazolin (500 mg/kg, Apotex, i.p.) were administered before surgery. Mice were anesthetized with isoflurane (4% induction, 1.5% maintenance). The bregma, lambda and sagittal sutures were exposed and a titanium headbar was secured to the frontal and parietal bones with cyanoacrylate glue and two screws. A 3 mm diameter craniotomy over the left whisker barrel cortex was performed while keeping the dura intact. The cranial window was then rinsed with saline to remove excess blood and the craniotomy covered with a glass coverslip plug (two 3 mm diameter and one 5 mm diameter glass coverslips stacked and glued together) and glued into place with cyanoacrylate glue. The glass window and the headbar were further secured with dental cement.

Cortical imaging

The cortex was imaged in awake mice. Three weeks after surgery, mice underwent several days of acclimation on a treadmill used in the imaging experiments. The treadmill allowed mice to move freely, reducing stress. Experiments were performed 3 to 13 weeks following surgery. Prior to an experimental session, mice were injected i.v. with 0.05 mL of 2.5% (W/V) Texas Red dextran (70,000 kDA, Sigma no. D1830) to label vessels for imaging. Mice were then secured by their headbar and imaged with a custom-built two-photon laser scanning (2 P) microscope based on a previous design[14] and a 16X, 0.8 NA objective (Nikon CF175 LWD 16xW).

Two-photon excitation of GCaMP6s and Texas Red dextran was achieved using a Ti:sapphire laser (Chameleon Vision, Coherent) tuned to 920 nm (30 to 65 mW post-objective laser power). Fluorescence was detected using bandpass emission filters (GCaMP6s, Chroma ET525/50m; Texas Red, Chroma ET630/75 m) and GaAsP photomultiplier tubes (H10770PA-40; Hamamatsu). Images (256×256 pixels) were acquired at 3.42 Hz, 30 to 155 μm below the cortical surface.

Analysis

Neuronal activity. GCaMP6s fluorescence expressed in neurons was measured in regions of interest (ROI) that encompassed most of the imaged frame. Multiple neuronal dendrites but few neuronal somata were

visible in the images (Figure 1(a) and (b)). Thus, the recorded fluorescence signal represented the activity of many neurons whose processes were adjacent to the imaged blood vessel. Neuronal somata and regions of the image where large vessels cast shadows were excluded from the fluorescence measurements. The neuronal response to a stimulus was taken as the peak of the fluorescence signal following stimulation divided by the baseline fluorescence before stimulus presentation. Trials where a mouse ran within the 5 s period before stimulus presentation were excluded from analysis. The whisker stimulus sometimes induced a startle response and/or running. These trials were not excluded as we have shown previously that such responses do not

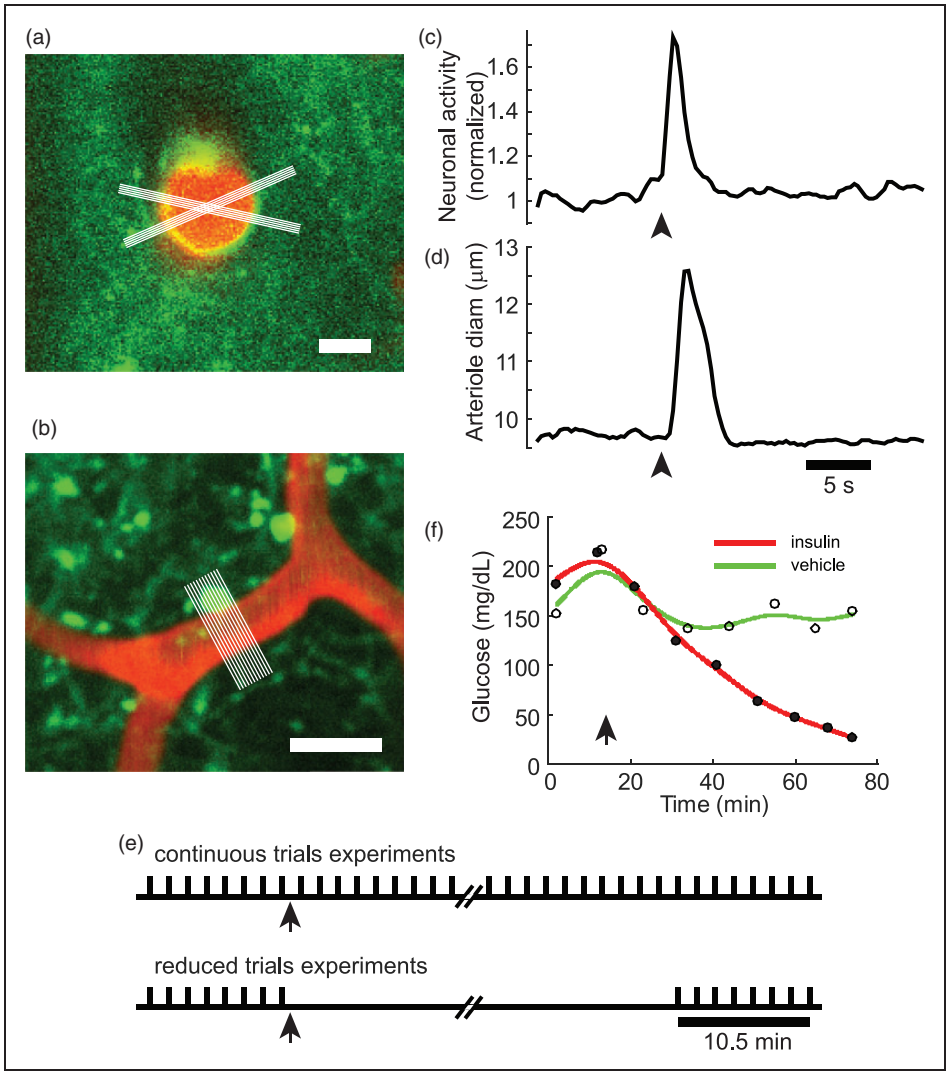

Figure 1. Measurement of neuronal activity, vessel diameter, and blood glucose. (a) Two-photon microscopy image of a Texas red dextran-labeled penetrating arteriole (red) and GCaMP6s-labeled neuronal processes (green) in the awake mouse cortex. White lines indicate locations where vessel diameter was measured. (b) Similar to (a), showing a 2nd order capillary. Scale bars in (a) and (b), 10 μm. (c) Neuronal response to a whisker stimulus (0.3 s air puff), as measured by the change in GCaMP6s fluorescence in neuronal processes, $(F + \Delta F)/F$. GCaMP6s fluorescence was measured over the entire field of the image. (d) Response of a penetrating arteriole to the same whisker stimulus as in (c). Arrowheads in (c) and (d) indicate the onset of the whisker stimulus. (e) Stimulus protocols employed. For "continuous trials experiments", trials were repeated every 90 s for the duration of an experiment, lasting from 55 to 90 min. Experiments were terminated when blood glucose fell below 20 mg/dL. For "reduced trials experiments", 8 consecutive 90 s trials were performed during euglycemic conditions, before insulin administration, and 8 additional trials during hypoglycemic conditions, when blood glucose fell below ~40 mg/dL. Vertical ticks represent individual stimulus trials; arrows indicate administration of insulin or vehicle. (f) Blood glucose levels during an experiment when insulin was administered (filled circles, red line) and a second control experiment when vehicle was administered (open circles, green line). Circles represent individual blood glucose measurements. The data are fit by a smoothing spline curve-fitting function. Arrow indicates the time of insulin or vehicle administration.

significantly alter stimulus-induced vessel dilation in penetrating arterioles and 2nd order capillaries.[15]

Vessel diameter. The diameters of Texas Red dextran-filled arterioles and capillaries (Figure 1(a) and (b)) were measured using a custom MATLAB routine. Vessel images were first registered to adjust for small movements of the brain in the X and Y planes (there was very little movement in the Z plane). The neuronal GCaMP6s images were then registered based on the vessel registration. When measuring the diameter of penetrating arterioles, which were viewed in cross-section, two sets of 9 lines, each set spanning 1.7 μm, were drawn at different angles across the arteriole diameter to account for potential asymmetries in vessel response (Figure 1(a)). The diameter of the arteriole was measured for each line crossing, as determined by taking the full width at half maximum of the intensity profile along the line using the MATLAB findpeaks function. All measured diameter values were then averaged. Capillaries were viewed en face. Only 2nd order capillaries were analyzed. Vessel order is defined as follows (see Figure 1(a) of Del Franco et al., 2022). Penetrating arterioles are vessels which branch off arteries at the surface of the brain and descend, more or less vertically, into the brain. First order capillaries branch off of these penetrating arterioles and 2nd order capillaries branch off of 1st order capillaries.[15–17] Capillary diameter was measured with a set of 39 lines spanning 3.7 μm and taken as the average of the diameter measurements for each line (Figure 1(b)). Responses of both arterioles and capillaries to a stimulus were taken as the peak diameter of the vessel following stimulation divided by the baseline vessel diameter before stimulus presentation. Latency to onset of stimulus-evoked vessel responses was taken as the first timepoint where vessel diameter rose from baseline to >15% of the peak amplitude.

Neurovascular coupling. Neurovascular coupling was quantified by two methods. In the first method, the value of neurovascular coupling was taken as the amplitude of the vessel response to a stimulus divided by the neuronal response to the stimulus. In the second method, the value of neurovascular coupling was taken as the amplitude of the convolution kernel describing the relation between neuronal activity and arteriole diameter during the full 30 s of an experimental trial. A similar approach has been used previously.[17,18] The kernel was calculated using multilinear ridge regression (ridge function, MATLAB), which is a form of linear regression where the coefficients are regularized, making it ideal for data where the variables are correlated. We used neural activity, as measured by Ca^{2+} fluorescence ($\Delta F/F$), as the independent variable, and vessel diameter as the dependent variable. The coefficients of the ridge regression correspond to the kernel which predicts vessel diameter from neural activity. The regression was trained on data from 15 s windows taken throughout each 30 s experimental trial. For the independent variable, we used changes in neuronal activity in 0.29 s increments over each 15 s window. For the dependent variable, we used the vessel diameter measured at the end of the 15 s window. Kernels were subsequently smoothed with a 1.5 s moving average filter (smooth function, MATLAB).

Sensory stimulation

The whiskers contralateral to the imaged cortex were stimulated with a 300 ms, 18 psi air puff directed onto the whiskers through a 15-gauge blunted needle. The needle was positioned ~3 mm in front of a mouse's snout and ~2 mm off the midline so that all whiskers on that side were stimulated to some extent. Note that the extent of whisker stimulation was not critical to our results as we are measuring the ratio of vascular to neuronal responses. Experimental trials were 30 s in duration, with the stimulus delivered after a 10 s pre-stimulus period. A series of 103 images were acquired during an experimental trial. Whisker stimulation consistently produced an increase in neuronal activity (Figure 1(c)) and vessel dilation (Figure 1(d)). Two stimulus protocols were used (Figure 1(e)). For "continuous trials experiments", trials were repeated every 90 s for the entire experiment, lasting from 55 to 90 min. For "reduced trials experiments", 8 consecutive 90 s trials were conducted during euglycemic conditions, before insulin administration, and 8 additional trials during hypoglycemic conditions, following insulin administration.

Induction of hypoglycemia and blood glucose monitoring

Insulin administration was used to induce hypoglycemia. Prior to an experiment, mice were fasted for 1.5 to 4 hours with water given ad libitum. After an initial series of stimulus trials, insulin glargine [3 U/kg, Sanofi # 00088-2220-33, 0.25 ml diluted 5X with saline vehicle containing glycerol and $ZnCl_2$[19]] was injected subcutaneously to induce hypoglycemia. In control experiments, the vehicle solution rather than insulin was injected. We have shown previously that insulin-induced hypoglycemia, rather than insulin itself, induces vascular changes. When glucose was co-administered with insulin to maintain euglycemia, vessels did not dilate.[13]

Blood glucose was measured at 5 to 15 min intervals throughout an experiment, with shorter intervals used

towards the end as glucose levels dropped more rapidly. Blood glucose was measured with a tail prick and a commercial veterinary blood glucose meter (AlphaTRAK 2, Zoetis). Blood glucose measured with tail pricks underestimates the glucose available to the brain via the arteriole circulation.[20] Blood glucose measurements reported in this study were not corrected for this difference in order to allow comparisons with other studies using tail prick measurements.

Experiments were terminated when blood glucose levels dropped below 20 mg/dL or when mice showed signs of distress. Following an experiment, animals were injected subcutaneously with 1 mL of 20% dextrose and allowed food ad libitum. A maximum of 3 insulin-induced hypoglycemia experiments were performed on individual mice with at least 7 days between experiments.

The blood glucose measurements made during an experiment were interpolated using a curve-fitting routine (fit function, smoothingspline option, MATLAB) in order to estimate blood glucose values at every point during an experiment (Figure 1(f)). A rise in blood glucose during the first 10 min of an experiment was typically observed and may have been due to the stress associated with handling, tail poke, or whisker stimulation. Insulin glargine, a long-acting form of insulin that works slowly, was used to produce hypoglycemia and blood glucose levels dropped slowly over a ~60 min period following administration (Figure 1(f)). Consequently, sets of 8 trials in the "reduced trials" protocol were acquired during periods when blood glucose was nearly constant.

Statistics

Experimental data were obtained from 5 male and 3 female mice for penetrating arteriole experiments and a separate set of 8 male and 1 female mice for capillary experiments. For each experimental group, data were combined across mice and across experimental sessions. Normality of datasets was determined using the one-sample Kolmogorov-Smirnov test (kstest function, 5% significance level, MATLAB). For normal data, significance was determined using one-way ANOVAs followed by Tukey's multiple comparison post hoc test. For data that was not normally distributed, the nonparametric Kruskal-Wallis test was used (kruskalwallis function, MATLAB). Data are given as mean ± SD in the text and in the figure plots. Numbers (n) are given as the number of vessels, mice, and the total number of experiments performed. The same vessel was typically imaged during several experiments. The number of vessels equaled the number of mice, as only one vessel was monitored per mouse. Samples were considered not significantly different (n.s.) for $p > 0.05$. When noted, outliers were removed using the rmoutliers, median option function, MATLAB.

Results

We assessed the effect of hypoglycemia on basal vessel diameter and neurovascular coupling in the cortex of awake mice. Neurovascular coupling was determined by simultaneously measuring the responses of neurons and blood vessels to whisker stimulation, with neuronal activity monitored by measuring the fluorescence of GCaMP6s-labeled neurons and vessel responses assessed by measuring the diameter of Texas Red-dextran filled penetrating arterioles and capillaries (Figure 1(a) to (d)). Hypoglycemia was induced by insulin administration (Figure 1(f)).

Basal arteriole diameter increases during hypoglycemia

We first measured the effect of hypoglycemia on the basal diameter of penetrating arterioles using the "continuous trials experiment" protocol (Figure 1(e)), with trials acquired every 90 s for the duration of the experiment. The arteriole diameter was tracked under euglycemic conditions, before insulin administration and under different degrees of hypoglycemia, following insulin administration. For the purposes of this study, we define euglycemia as 150–70 mg/dL, mild hypoglycemia as 70–54 mg/dL, moderate hypoglycemia as 54–35 mg/dL, and severe hypoglycemia as <35 mg/dl blood glucose.

Under euglycemic conditions, the basal diameter of penetrating arterioles in the barrel cortex averaged 13.2 ± 2.5 μm (mean ± SD; 8 vessels in 8 mice, 18 experiments), measured at depths ranging from 36 to 73 μm beneath the pial surface (mean ± SD depth, 54.0 ± 10.8 μm).

For each trial, arteriole diameter values were normalized to the mean value under euglycemia in order to compare changes in diameter between vessels under different glycemic conditions. Basal arteriole diameter increased as blood glucose diminished following insulin administration (Figure 2(a) and (b)). Compared to euglycemia, basal vessel diameter increased by 1.5 ± 5.3% (n.s.), 5.2 ± 8.8% ($p < 0.001$), and 10.3 ± 8.8% ($p < 0.001$; mean ± SD; Kruskal-Wallis) under mild, moderate and severe hypoglycemia, respectively (Figure 2(b)). As seen in Figure 2(a), basal diameter rose as blood glucose dropped below ~35 mg/dL. The threshold glycemic level for dilation in some vessels was very sharp. This is illustrated in the inset in Figure 2(a), which shows a record of the diameter of an individual vessel in a single experiment during insulin-induced

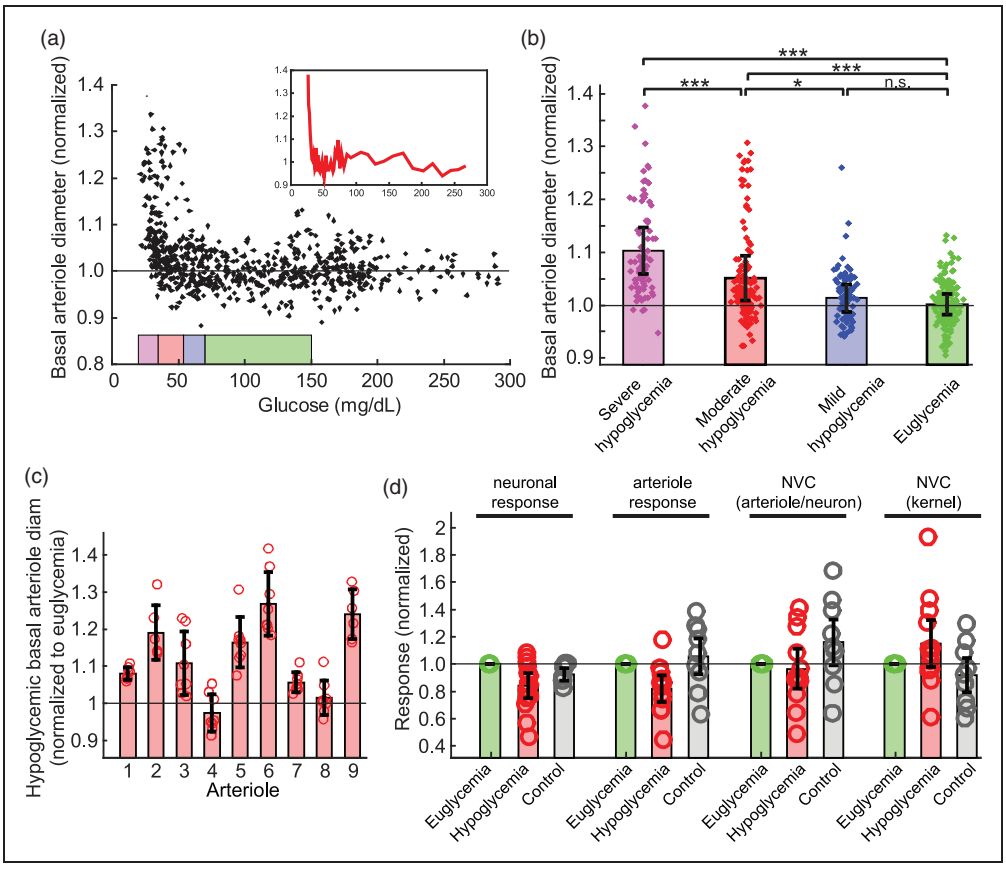

Figure 2. Responses of penetrating arterioles, neurons, and neurovascular coupling to whisker stimulation during euglycemia and hypoglycemia. (a) Basal arteriole diameter during insulin-induced hypoglycemia. Data points (black circles) represent individual arteriole diameter measurements. Data are normalized to the mean of all arteriole diameter measurements during euglycemia for each experiment. Colored rectangles at the bottom indicate glycemic ranges [color scale the same as in (b)]. Combined data from 8 vessels in 8 mice, 15 experiments. Inset: red line plots the diameter vs glycemic level for a single experiment on a single arteriole. Axes are the same as the main figure. (b) Summary of the results in (a), with data binned into 4 glycemic ranges (euglycemia, 70–150; mild hypoglycemia, 54–70; moderate hypoglycemia, 35–54; and severe hypoglycemia, 20–35 mg/dL). Data for trials where blood glucose was >150 mg/dL were omitted. Individual measurements, mean ± SD, n = 8 vessels in 8 mice, 15 experiments; *, $p < 0.05$; ***, $p < 0.001$; n.s. not significant. (c) Basal arteriole diameter during hypoglycemia (20 to 44 mg/dL) with data normalized to the mean diameters during euglycemia (70–150 mg/dL). Responses of 9 arterioles are shown. Individual measurements, mean ± SD, n = 9 vessels, 9 mice. 20 of the 36 pairwise comparisons between vessels are significantly different. (d) Summary of responses to whisker stimulation. For each experiment, responses are normalized to the mean of the responses during euglycemia. Neuronal responses represent the peak change in the amplitude of GCaMP6s fluorescence in neuronal processes. Arteriole responses represent the peak change in the arteriole diameter. NVC (arteriole/neuron) represents a measure of neurovascular coupling as calculated by the ratio of the arteriole response to the neuronal response for each stimulus trial. NVC (kernel) represents a measure of neurovascular coupling, as calculated by the peak amplitude of the convolution kernel relating the neuronal response to the vessel response, calculated for each stimulus trial. Outliers were removed for panel (d) calculations (see Methods). None of the responses measured during hypoglycemia are significantly different from the euglycemia or control responses. Mean ± SD, n = 9 vessels in 9 mice.

hypoglycemia. In this experiment, the arteriole diameter remained nearly constant until blood glucose dropped below 32 mg/dL, at which point the vessel dilated rapidly.

As illustrated in Figure 2(b), there was a great deal of variability in the diameters of arterioles under hypoglycemic conditions. To determine whether this variability was due to a differential responsiveness of different vessels to hypoglycemia, we plotted the normalized basal vessel diameter for each vessel imaged during hypoglycemia (Figure 2(c)). There was a great deal of variability in the responses of individual vessels to hypoglycemia. Of the 36 pairwise comparisons between vessels, 20 were significantly different from each other ($p < 0.05$, one-way ANOVA), demonstrating that different arterioles respond differently to hypoglycemia. Note that only one vessel was imaged per mouse. Thus, the dataset does not allow us to

determine whether the differential vessel responsiveness was due to differences between vessels or between mice.

The absolute change in basal vessel diameter during hypoglycemia was also determined. The mean diameter of all vessels sampled increased from $13.2 \pm 2.5\,\mu m$ during euglycemia (70–150 mg/dL) to $14.8 \pm 3.2\,\mu m$ during hypoglycemia (20 to 44 mg/dL), resulting in a mean hypoglycemia-induced dilation of $1.6\,\mu m$. Dilations ranged from -0.4 to $3.9\,\mu m$ for different vessels.

Neuron and arteriole responses are unchanged during hypoglycemia

We monitored both neuronal and arteriole responses to whisker stimulation during euglycemia and hypoglycemia. Stimulation of the contralateral whiskers evoked rapid, transient responses (Figure 1(c) and (d)). The neuronal response peaked rapidly while the arteriole response developed with a longer latency and peaked later. The neuronal response to whisker stimulation during euglycemia, measured as an increase in GCaMP6s fluorescence, equaled $82.6 \pm 11.9\%$ (mean $\pm$ SD, $n = 8$ vessels in 8 mice, 18 experiments). The increase in arteriole diameter equaled $17.4 \pm 3.0\%$ (mean $\pm$ SD, $n = 8$ vessels in 8 mice, 18 experiments).

In initial experiments, we stimulated the whiskers in a continuous series of trials (continuous trials protocol; Figure 1(e), top). In control experiments, where vehicle was administered, we found that the amplitude of the neuronal response declined over time. Fifty-five min into an experiment, the neuronal response was reduced by $31 \pm 10\%$ (mean $\pm$ SD, $n = 8$ experiments). This decline was likely due, at least in part, to habituation to the stimulus, as the degree of decline was reduced, but not eliminated, when a "reduced trials" protocol was employed (Figure 1(e), bottom). In this protocol, 8 trials were acquired at the beginning of an experiment to measure the initial response to whisker stimulation. 45 min later, an additional 8 trials were acquired. In control experiments using this "reduced trials" protocol, neuronal responses at the end of the experiment were reduced by only $7.3 \pm 6.6\%$ (mean $\pm$ SD, $n = 10$ experiments).

In order to minimize habituation, we chose to assess the effects of hypoglycemia on neuronal and arteriole responses and on neurovascular coupling using the "reduced trials" protocol. Responses under euglycemic conditions were assessed in 8 trials before insulin administration. Following insulin administration, blood glucose levels were tracked and an additional 8 trials were acquired after blood glucose levels dropped below ~40 mg/dL. This occurred, on average, 45 min after insulin administration. The mean values of the hypoglycemic trials were then compared to the mean values of the euglycemic trials. Blood glucose levels during hypoglycemia trials averaged 32.1 ± 8.0 mg/dL (mean $\pm$ SD, $n = 18$ experiments) and ranged from 20 to 44 mg/dL.

Results of these "reduced trials" experiments are summarized in Figure 2(d). Neither neuronal responses nor arteriole responses differed significantly during hypoglycemia, compared to responses acquired during euglycemia. Neuronal responses during hypoglycemia were $15.7 \pm 17.3\%$ smaller than during euglycemia (mean $\pm$ SD; n.s., $n = 8$ vessels in 8 mice, 9 experiments). The observed reduction was likely due, at least in part, to habituation rather than the lowered glycemic level as control neuronal responses (acquired 45 min after vehicle injection) were also smaller ($7.3 \pm 6.6\%$ reduction, n.s., $n = 8$ vessels in 8 mice, 10 experiments). Arteriole responses to whisker stimulation during hypoglycemia were also smaller than during euglycemia ($19.9 \pm 17.6\%$ reduction; mean $\pm$ SD; n.s., $n = 8$ vessels in 8 mice, 9 experiments). Control arteriole responses were $5.8 \pm 24.6\%$ larger (mean $\pm$ SD; n.s., $n = 8$ vessels in 8 mice, 10 experiments).

Arteriole neurovascular coupling is unchanged during hypoglycemia

Arteriole/neuron response ratio. Neurovascular coupling was quantified by two measures. In the first method, neurovascular coupling was calculated as the peak amplitude of the arteriole response to whisker stimulation divided by the peak amplitude of the neuronal response. We found that neurovascular coupling did not change during hypoglycemia. Both hypoglycemic and control neurovascular coupling ratios were not significantly different compared to the euglycemic ratio (Figure 2(d); $3.7 \pm 27.6\%$ reduction and $16.1 \pm 32.2\%$ increase, respectively; n.s., $n = 8$ vessels in 8 mice, 9 and 10 experiments, respectively).

Kernel amplitude. A second measure of neurovascular coupling was calculated by computing the convolution kernel relating the non-normalized neuronal response to the non-normalized arteriole response during each 30 s trial and comparing kernel amplitudes. As discussed below, this kernel is similar, but not the same, as the hemodynamic response function utilized in fMRI studies.

The relation between the neuronal and vascular responses to whisker stimulation and the convolution kernel is illustrated in Figure 3. The time course of the arteriole response was noticeably slower than that of the neuronal response, with longer onset and peak times (Figure 3(a)). The transient vessel dilation was followed by a small, slower constriction. A similar dip was not seen in the neuronal response. The time

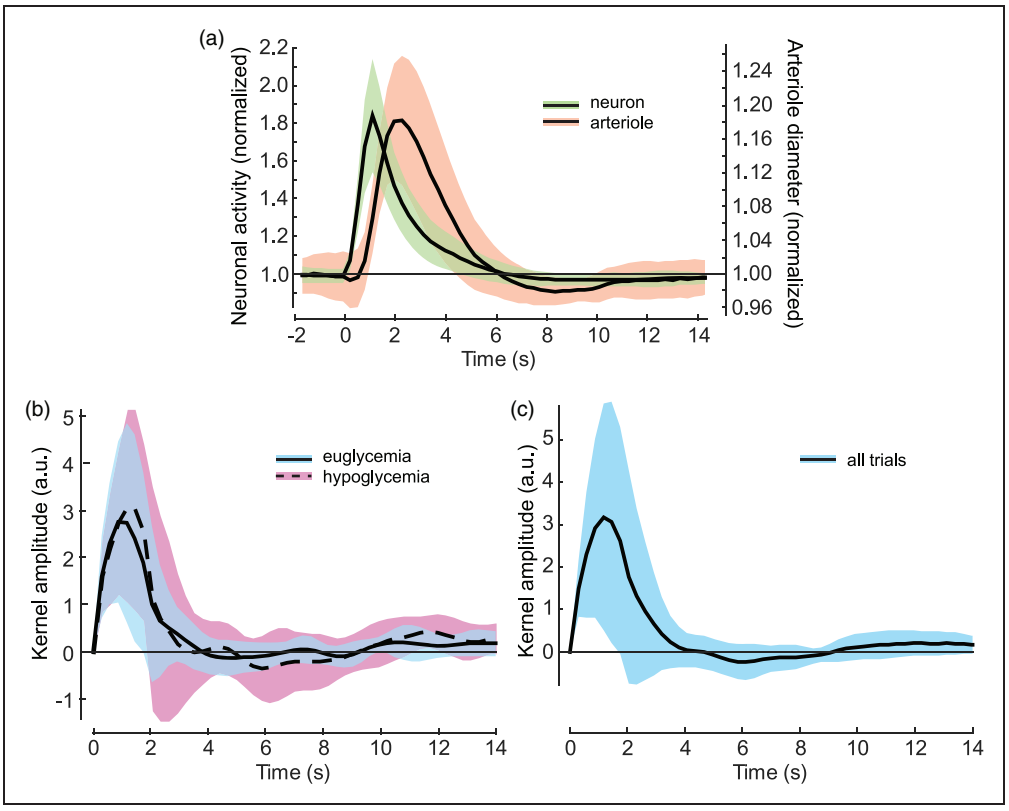

Figure 3. Convolution kernels relating the neuronal response to the arteriole response evoked by whisker stimulation. (a) Normalized neuronal and arteriole responses to whisker stimulation. Each response is the mean ± SD of 8 vessels in 8 mice, 18 experiments. Multiple trials were averaged for each experiment. Stimulus onset at time = 0 s. (b) Convolution kernels for euglycemia and hypoglycemia trials (mean ± SD; 8 vessels in 8 mice, 9 experiments for each trace). The kernels represent the relation between the non-normalized neuronal response and the non-normalized vessel response for each trial. (c) Same as (b) except that the kernel is calculated from all euglycemia, hypoglycemia and control trials (mean ± SD, 8 vessels in 8 mice, 18 experiments). a.u.: arbitrary units.

course of the vascular response was compared under different glycemic conditions. The latency to onset of the stimulus-evoked response did not differ between euglycemia and hypoglycemia (0.77 ± 0.15 s vs 0.81 ± 0.13 s, n.s., n = 8 vessels in 8 mice, 9 experiments for each). However, the latency to peak increased during hypoglycemia (1.83 ± 0.35 s vs 2.19 ± 0.83, $p < 0.005$, one-way ANOVA). The sampling rate of our image dataset (3.42 Hz) was not high enough to accurately measure the latencies of the neuronal responses.

The differences between the time courses of the neuronal and vascular responses to whisker stimulation are reflected in the kernels calculated under euglycemic and hypoglycemic conditions (Figure 3(b)). Both kernels show a transient peak followed by a delayed undershoot. The amplitudes of the euglycemic and hypoglycemic kernels did not differ significantly from each other or from the control kernel (Figure 2(d)). Kernel amplitude was 15.2 ± 33.8% larger during hypoglycemia and 7.9 ± 23.3% smaller during controls, compared to euglycemia (mean ± SD; n.s., n = 8 vessels in 8 mice, 9 experiments for each, one-way ANOVA), which was calculated from trials at the beginning of each experiment. In addition, the latencies to the peak of the kernels did not differ significantly between euglycemia and hypoglycemia responses (0.94 ± 0.35 s vs 1.36 ± 0.60 s; mean ± SD; n.s., n = 8 vessels in 8 mice, 9 experiments for each, one-way ANOVA). Although the hypoglycemia kernel trended larger than the control kernel (Figures 2(d) and 3(b)), the opposite trend was seen in the arteriole/neuron response ratio, where the hypoglycemia value trended lower than the euglycemia value (Figure 2(d)). Thus, the two measures of neurovascular coupling did not show a consistent trend.

As there were no significant differences between the kernels calculated for euglycemia, hypoglycemia and control trials, data from all trials were pooled to calculate a kernel having increased precision for comparison to the hemodynamic response function (see below). The kernel peaked at 1.20 ± 0.33 s (mean ± SD of 8 vessels in 8 mice, 18 experiments), reflecting

the delay between the neuronal and vascular responses (Figure 3(c)). The kernel also had a delayed undershoot which peaked at 6.1 s, reflecting the delayed constriction seen in the vascular responses.

Basal capillary diameter increases during hypoglycemia

The effect of hypoglycemia on the basal diameter of capillaries and on capillary neurovascular coupling was also determined. Responses were measured for 2nd order capillaries, identified as described in Methods. The "reduced trials" protocol (Figure 1(e), bottom) was employed for all capillary experiments; 8 trials were acquired under euglycemic conditions and then, following insulin injection, 8 additional trials were acquired as blood glucose dropped below ~40 mg/dL.

Under euglycemia, the average basal diameter of 2nd order capillaries was 5.26 ± 0.42 μm (mean ± SD; 9 vessels in 9 mice, 34 experiments), measured at depths ranging from 62 to 156 μm beneath the pial surface (mean depth, 99.2 ± 23.6 μm, mean ± SD).

Basal capillary diameter increased as blood glucose diminished following insulin administration (Figure 4 (a) and (b)). Because a "reduced trials" protocol was utilized, capillary diameter was not determined during mild hypoglycemia. However, basal diameter increased significantly during moderate and severe hypoglycemia. Compared to euglycemia, basal vessel diameter increased by $5.4 \pm 7.5\%$ ($p < 0.001$), and $9.7 \pm 7.5\%$ ($p < 0.001$; mean ± SD; 9 vessels in 9 mice, 19 experiments; one-way ANOVA) under moderate and severe hypoglycemia, respectively (Figure 4(b)). The basal diameter of 2nd order capillaries rose rapidly as blood glucose dropped below ~35 mg/dL. This is illustrated in the inset in Figure 4(a), which shows a record of the diameter of an individual vessel in a single experiment during insulin-induced hypoglycemia. In this experiment, the arteriole diameter remained nearly constant until blood glucose dropped below 30 mg/dL, at which point the vessel dilated rapidly.

As illustrated in Figure 4(b), there was a great deal of variability in the diameter of capillaries under hypoglycemic conditions. To determine whether this variability was due to a differential responsiveness of different vessels to hypoglycemia, we plotted the normalized basal vessel diameter for each vessel imaged (Figure 4(c)). There was a great deal of variability in the responses of individual vessels to hypoglycemia. Of the 36 pairwise comparisons between vessels, 17 were significantly different from each other ($p < 0.05$, one-way ANOVA), demonstrating that different capillaries respond differently to hypoglycemia.

The absolute change in basal capillary diameter during hypoglycemia was also determined. The mean diameter of all vessels sampled increased from 5.26 ± 0.42 μm during euglycemia (70–150 mg/dL) to 5.70 ± 0.66 μm during hypoglycemia (20 to 44 mg/dL), resulting in a mean hypoglycemia-induced dilation of 0.44 μm. Dilations ranged from −0.10 to 0.79 μm for different vessels.

Capillary responses are unchanged during hypoglycemia

Capillary responses to whisker stimulation did not vary significantly between euglycemic and hypoglycemic conditions (Figure 4(d)). During euglycemia, stimuli evoked dilations of $5.2 \pm 0.4\%$ (mean ± SD, n = 9 vessels in 9 mice, 34 experiments). This diameter increase did not differ significantly during hypoglycemia ($11.6 \pm 32.1\%$ reduction compared to euglycemia, n.s., mean ± SD, n = 19 experiments) and following control vehicle injection ($7.3 \pm 31.5\%$ reduction, mean ± SD, n.s., n = 15 experiments, one-way ANOVA). Similarly, neuronal responses to whisker stimulation did not change during hypoglycemia (Figure 4(d); $11.2 \pm 17.2\%$ reduction compared to euglycemia, mean ± SD, n.s., n = 19 experiments) and following control vehicle injection ($19.0 \pm 22.0\%$ reduction, n.s., mean ± SD, n = 15 experiments, one-way ANOVA).

Capillary neurovascular coupling is unchanged during hypoglycemia

Neurovascular coupling at 2nd order capillaries was quantified using the same two measures employed to compute arteriole neurovascular coupling: the ratio of the peak amplitude of the capillary response to the peak amplitude of the neuronal response and the convolution kernel relating the two responses. Both methods demonstrated that capillary neurovascular coupling did not change during hypoglycemia.

The relation between the neuronal and capillary responses to whisker stimulation and the convolution kernel is illustrated in Figure 5. The time course of the capillary response was noticeably slower than that of the neuronal response, with longer onset and peak times (Figure 5(a)). In contrast to the arteriole response, the capillary response did not display a delayed constriction following the transient dilation. The time course of the capillary response was compared under different glycemic conditions. The latency to onset of the stimulus-evoked response did not differ between euglycemia and hypoglycemia (0.90 ± 0.29 s vs 1.04 ± 0.31 s, n.s., n = 8 vessels in 8 mice, 9 experiments for each). Nor did the latency to peak change during hypoglycemia (2.00 ± 0.43 s vs 2.30 ± 0.63, n.s., one-way ANOVA).

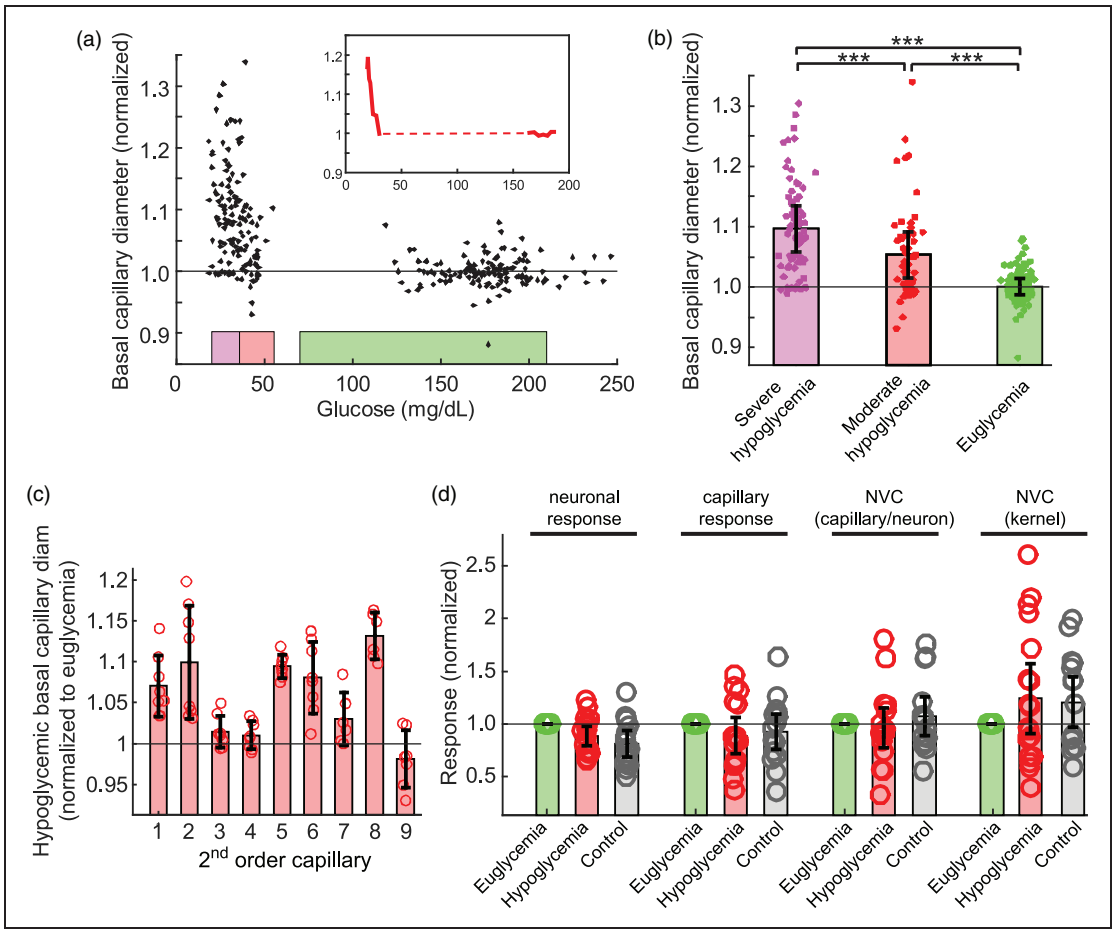

Figure 4. Responses of 2nd order capillaries, neurons, and neurovascular coupling to whisker stimulation during euglycemia and hypoglycemia. (a) Basal capillary diameter during insulin-induced hypoglycemia. Data points (black circles) represent individual capillary diameter measurements. Data are normalized to the mean of all capillary diameter measurements during euglycemia for each experiment. Colored rectangles at the bottom indicate glycemic ranges [color scale the same as in (b)]. Combined data from 9 vessels in 9 mice, 19 experiments. Inset: solid red line plots diameter vs glycemic level for a single experiment on a single capillary. Dashed line spans the glycemic range that was not measured. Axes are the same as in the main figure. (b) Summary of the results in (a), with data binned into 3 glycemic ranges (euglycemia, 70–210; moderate hypoglycemia, 35–54; and severe hypoglycemia, 20–35 mg/dL). Data for blood glucose >210 mg/dL were omitted. Individual measurements, mean $\pm$ SD. n $=9$ vessels in 9 mice, 19 experiments. ***, $p<0.001$. In panels (a) and (b), measurements were not made during mild hypoglycemia. (c) Basal capillary diameter during hypoglycemia (20 to 44 mg/dL) with data normalized to the mean diameters during euglycemia (70–150 mg/dL). Responses of 9 capillaries are shown. Individual measurements, mean $\pm$ SD, n $=9$ vessels, 9 mice. 17 of the 36 pairwise comparisons between vessels are significantly different. (d) Summary of responses to whisker stimulation. For each experiment, responses are normalized to the mean of the responses during euglycemia. Response groups are the same as in Figure 2. Outliers were removed for panel (d) calculations (see Methods). None of the responses measured during hypoglycemia are significantly different from the euglycemia or control responses.

The differences between the time courses of the neuronal and vascular responses to whisker stimulation are reflected in the kernels calculated under euglycemic and hypoglycemic conditions (Figure 5(b)). Both kernels show a transient peak but no delayed undershoot. The amplitudes of the euglycemic and hypoglycemic kernels did not differ significantly from each other or from the control kernel (Figure 4(d)). Kernel amplitude was $24.9 \pm 64.5\%$ larger during hypoglycemia and $20.5 \pm 45.6\%$ larger during controls, compared to euglycemia, which was calculated from trials at the beginning of each experiment (mean $\pm$ SD; n.s., n $=9$ mice, 19 and 15 experiments, respectively, one-way ANOVA). In addition, the latencies to the peak of the kernels did not differ significantly between euglycemia and hypoglycemia trials (1.85 ± 2.58 vs 1.67 ± 2.61 s; mean $\pm$ SD; n.s., n $=9$ mice, 19 experiments for each, one-way ANOVA). As in the analysis of arteriole neurovascular coupling, the capillary hypoglycemia kernel trended larger than the control kernel

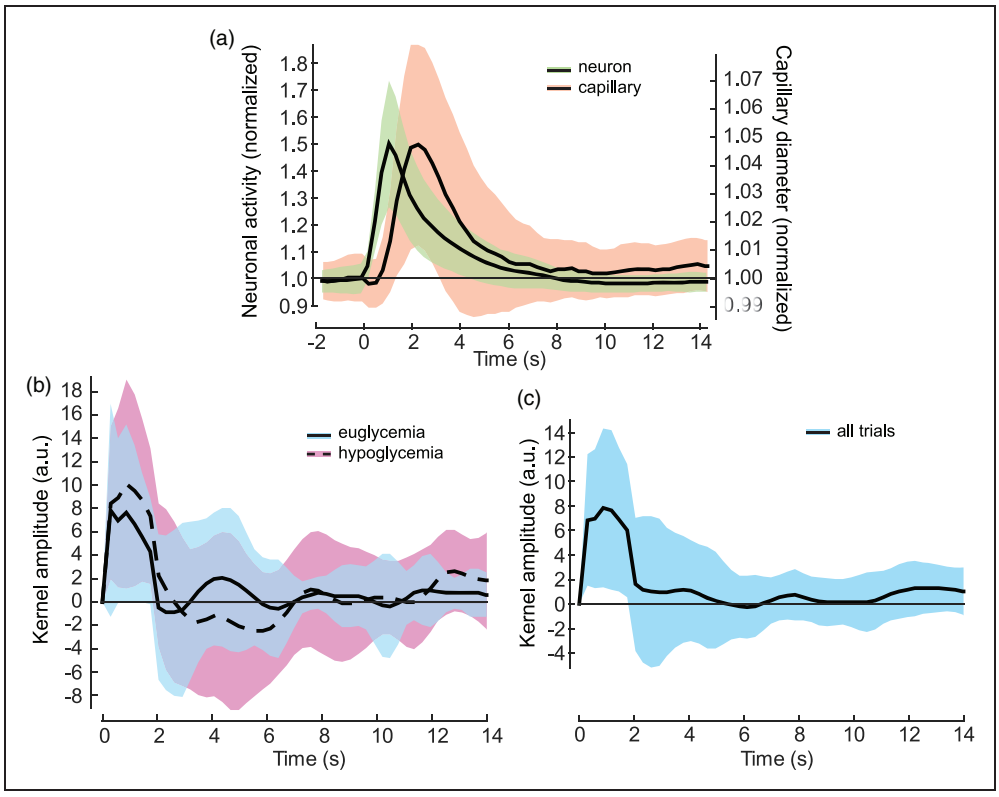

Figure 5. Convolution kernels relating the neuronal response to the capillary response evoked by whisker stimulation. (a) Normalized neuronal and capillary responses to whisker stimulation. Each response is the mean ± SD of 9 vessels in 9 mice, 34 experiments. Multiple trials were averaged for each experiment. Stimulus onset at time = 0 s. (b) Convolution kernels for euglycemia and hypoglycemia trials (mean ± SD; 9 vessels in 9 mice, 19 experiments for each trace). The kernels represent the relation between the non-normalized neuronal response and the non-normalized vessel response for each trial. (c) Same as (b) except that the kernel is calculated from all euglycemia, hypoglycemia and control trials (mean ± SD, 9 vessels in 9 mice, 34 experiments). a.u.: arbitrary units.

(Figures 4(d) and 5(b)), and the opposite trend was seen in the arteriole/neuron response ratio, where the hypoglycemia value trended lower than the euglycemia value (Figure 4(d)).

As there were no significant differences between the kernels calculated for euglycemia, hypoglycemia and control trials, data from all trials were pooled to calculate a kernel having increased precision (Figure 5(c)). The kernel peaked at 1.76 ± 2.72 s (mean ± SD, 9 vessels in 9 mice, 34 experiments) and did not show a delayed negative phase.

Discussion

We have characterized neurovascular coupling in the barrel cortex of the mouse during insulin-induced hypoglycemia. Neurovascular coupling was quantified by two measures: the ratio of vascular to neuronal responses and the convolution kernel relating the two responses. We found, by both measures, that neurovascular coupling remained unchanged during hypoglycemia. That is, for a given neuronal response to a stimulus, similar vascular responses were evoked during euglycemia and hypoglycemia. This held true at both penetrating arterioles and 2nd order capillaries. These results demonstrate that neurovascular coupling is maintained as an important physiological mechanism for enhancing the supply of glucose to active neurons during hypoglycemia, when it is critically needed. These findings further show that neurovascular coupling is independent of basal vessel diameter, as has been observed previously in hypercapnia-[21,22] and acetazolamide-induced[23] vessel dilation.

These findings shed light on previous reports of hypoglycemia-induced blood flow changes in the brain. fMRI studies in humans[7–9] and rats,[11] showed that fMRI responses to sensory stimulation, motor action, and nerve stimulation were reduced during hypoglycemia. These decreases, indicating reductions in the blood flow responses evoked by stimulation, could be due to decreases in neurovascular coupling during hypoglycemia. Neuronal activity was not monitored in these studies, however, and one should keep in mind that changes in basal CBF, which occur during hypoglycemia, can influence the magnitude of fMRI responses.[24] Pertinent to this question, an investigation

measuring regional CBF in humans with positron emission tomography[12] found no change in the CBF response to tactile stimulation during hypoglycemia. Our results highlight the importance of quantitatively assessing both neuronal activity and vascular responses when evaluating the neurovascular coupling response.

The maintenance of neurovascular coupling during reduced glycemic levels demonstrates the robustness of the homeostatic response. This has been demonstrated previously under other non-physiological conditions; neurovascular coupling is maintained during hyperoxia[25] and hypercapnia.[21,22] Neurovascular coupling is also maintained during some pathological conditions, including Parkinson's disease,[26] but not during Alzheimer's disease[27] and amyotrophic lateral sclerosis,[28,29] where it is reduced.

Our results show, in addition, that in the awake mouse, stimulus-evoked neuronal activity is not diminished during hypoglycemia, even during severe hypoglycemia. To our knowledge, these are the first direct measurements of stimulus-evoked neuronal activity under hypoglycemic conditions. In line with this observation, studies in humans[30] and cats[31] demonstrated no hypoglycemia-induced decreases in the visual evoked potential and the auditory evoked potential, although resting EEG amplitudes were decreased. These studies suggest that hypoglycemia may reduce neuronal activity in higher cortical centers, but not stimulus-evoked neuronal responses in primary sensory areas.

In addition to neurovascular coupling, hypoglycemia-induced changes to basal vessel diameter were characterized. We found that in both penetrating arterioles and 2nd order capillaries, the basal diameter of vessels began to increase during moderate hypoglycemia and dilated further during severe hypoglycemia. Individual arterioles and capillaries displayed a threshold hypoglycemic level of 30 to 35 mg/dL below which point vessels dilated rapidly. Although the hypoglycemia-induced arteriole and capillary dilations we observed were small (10.3%, 1.6 μm absolute dilation in arterioles and 9.7%, 0.44 μm absolute dilation in capillaries) these dilations can lead to substantial blood flow increases. According to the 4th power Hagen-Poiseuille relation, 10.3 and 9.7% vessel diameter increases result in 48 and 45% increases in blood flow through the vessels. Actual increases in capillaries can be even larger, as vessel resistance increases beyond the 4th power relation in capillaries smaller than 5 μm in diameter.[32] It is interesting to note that the glucose uptake rate into the brain rises rapidly once blood glucose drops below ~36 mg/dL,[33] a similar threshold level as we observed for hypoglycemia-induced vessel dilation.

These results confirm our previous finding that the basal diameter of arterioles dilates during hypoglycemia.[13] The results demonstrate that the dilation of both arterioles and capillaries contributes to the increases in CBF that occur during hypoglycemia.[34–36] This basal blood flow increase is an essential component of the response to hypoglycemia, increasing the supply of glucose to the hypoglycemic brain.

We also measured the latency to the onset and peak of stimulus-evoked vascular responses, finding that arterioles responded faster than 2nd order capillaries, with onset latencies of ~0.79 and ~0.95 s, respectively. These findings are in agreement with a recent study in the mouse barrel cortex which found that penetrating arteriole responses to whisker stimulation were faster than 2nd order capillary responses.[17]

Insulin-induced hypoglycemia triggers a counter-regulatory response which leads to increases in systemic glucagon and adrenaline levels.[37] Although the counter-regulatory response was not monitored in this study, changing hormone levels, particularly adrenaline, which increases cerebral blood flow,[38] could influence cerebral vascular diameter.

We calculated the convolution kernel relating neuronal and vascular responses as one method of evaluating neurovascular coupling. The arteriole and capillary kernels both displayed a rapid positive component while the arteriole kernel also showed a secondary, slow negative component. The positive component of the kernels corresponds to vessel dilation evoked by neuronal activity, which is due to the release of vasodilatory chemicals from neurons and/or astrocytes.[2,3] The negative component of the kernel observed in arterioles corresponds to the secondary constriction of arterioles (Figure 3(a)), which could be due to the action of a vasoconstrictor such as 20-HETE.[39,40] Alternately, it could be due to an intrinsic response of the arteriole to an increase in vessel pressure or shear stress due to increased perfusion.[41]

The convolution kernels we computed resemble the hemodynamic response functions that have been derived to describe the relation between neuronal activity and CBF, measured with fMRI[42,43] and optical methods.[18,44] Both the kernel and the hemodynamic response function show transient positive phases followed by a slower negative phase, which we observed for arterioles but not capillaries. The two responses are not identical, however. The components of the kernels computed in this study are more rapid than those of the hemodynamic response function. The arteriole kernel peaked at 1.2 s and the secondary negative component at 6.1 s while the hemodynamic response function peaks at ~7 s and has a secondary negative phase peaking between 10 to 20 s.

Overall, our results demonstrate that during hypoglycemia, neurovascular coupling is unaltered and arterioles and capillaries experience tonic dilation. Both of these physiological responses contribute to increased

glucose supply to active neurons when plasma glucose levels are reduced.

Funding

The author(s) disclosed receipt of the following financial support for the research, authorship, and/or publication of this article: Supported by National Institutes of Health Grants R01 NS-126166, and P30 EY-011374 to EAN and by National Institutes of Health Grants T32 EY025187 and F31 DK116498 to ARN.

Declaration of conflicting interests

The author(s) declared no potential conflicts of interest with respect to the research, authorship, and/or publication of this article.

Authors' contributions

EAN and ARN designed the research; PPC and EAN performed the research; EAN analyzed the data; EAN wrote the manuscript.

Availability of data and materials

The data that support the findings of this study and the MATLAB routines used to analyze the data are available from the corresponding author upon reasonable request.

References

1. Raichle ME. The restless brain: how intrinsic activity organizes brain function. *Phil Trans R Soc B* 2015; 370: 20140172.
2. Attwell D, Buchan AM, Charpak S, et al. Glial and neuronal control of brain blood flow. *Nature* 2010; 468: 232–243.
3. Iadecola C. The neurovascular unit coming of age: a journey through neurovascular coupling in health and disease. *Neuron* 2017; 96: 17–42.
4. Johnson-Rabbett B and Seaquist ER. Hypoglycemia in diabetes: the dark side of diabetes treatment. A patient-centered review. *J Diabetes* 2019; 11: 711–718.
5. Languren G, Montiel T, Julio-Amilpas A, et al. Neuronal damage and cognitive impairment associated with hypoglycemia: an integrated view. *Neurochem Int* 2013; 63: 331–343.
6. Cryer PE. Severe hypoglycemia predicts mortality in diabetes. *Diabetes Care* 2013; 36: e61–1816.
7. Heptulla RA, Anderson AW, Jones TW, et al. Hypoglycemia reduces the fMRI response to visual stimulation in the human brain. *Diabetes* 1999; 48: SA55.
8. Anderson AW, Heptulla RA, Driesen N, et al. Effects of hypoglycemia on human brain activation measured with fMRI. *Magn Reson Imaging* 2006; 24: 693–697.
9. Driesen NR, Goldberg PA, Anderson AW, et al. Hypoglycemia reduces the blood-oxygenation level dependent signal in primary auditory and visual cortex: a functional magnetic resonance imaging study. *J Neurosci Res* 2007; 85: 575–582.
10. Rosenthal JM, Amiel SA, Yágüez L, et al. The effect of acute hypoglycemia on brain function and activation. A functional magnetic resonance imaging study. *Diabetes* 2001; 50: 1618–1626.
11. Kennan RP, Jacob RJ, Sherwin RS, et al. Effects of hypoglycemia on functional magnetic resonance imaging response to median nerve stimulation in the rat brain. *J Cereb Blood Flow Metab* 2000; 20: 1352–1359.
12. Powers WJ, Hirsch IB and Cryer PE. Effect of stepped hypoglycemia on regional cerebral blood flow response to physiological brain activation. *Am J Physiol* 1996; 270: H554–H559.
13. Nippert AR, Chiang P-P, Del Franco AP, et al. Astrocyte regulation of cerebral blood flow during hypoglycemia. *J Cereb Blood Flow Metab* 2022; 42: 1534–1546.
14. Rosenegger DG, Tran CH, LeDue J, et al. A high performance, cost-effective, open-source microscope for scanning two-photon microscopy that is modular and readily adaptable. *PLoS One* 2014; 9: e110475.
15. Del Franco AP, Chiang P-P and Newman EA. Dilation of cortical capillaries is not related to astrocyte calcium signaling. *Glia* 2022; 70: 508–521.
16. Dalkara T, Gursoy-Ozdemir Y and Yemisci M. Brain microvascular pericytes in health and disease. *Acta Neuropathol* 2011; 122: 1–9.
17. Rungta RL, Zuend M, Aydin A-K, et al. Diversity of neurovascular coupling dynamics along vascular arbors in layer II/III somatosensory cortex. *Commun Biol* 2021; 4: 855.
18. Winder AT, Echagarruga C, Zhang Q, et al. Weak correlations between hemodynamic signals and ongoing neural activity during the resting state. *Nat Neurosci* 2017; 20: 1761–1769.
19. Stammberger I, Bube A, Durchfeld-Meyer B, et al. Evaluation of the carcinogenic potential of insulin glargine (LANTUS) in rats and mice. *Int J Toxicol* 2002; 21: 171–179.
20. Chan YK, Davis PF, Poppitt SD, et al. Influence of tail versus cardiac sampling on blood glucose and lipid profiles in mice. *Lab Anim* 2012; 46: 142–147.
21. Kennerley AJ, Harris S, Bruyns-Haylett M, et al. Early and late Stimulus-Evoked cortical hemodynamic responses provide insight into the neurogenic nature of neurovascular coupling. *J Cereb Blood Flow Metab* 2012; 32: 468–480.
22. Maggio P, Salinet ASM, Panerai RB, et al. Does hypercapnia-induced impairment of cerebral autoregulation affect neurovascular coupling? A functional TCD study. *J Appl Physiol (1985)* 2013; 115: 491–497.
23. Yonai Y, Boms N, Molnar S, et al. Acetazolamide-induced vasodilation does not inhibit the visually evoked flow response. *J Cereb Blood Flow Metab* 2010; 30: 516–521.
24. Cohen ER, Ugurbil K and Kim S-G. Effect of basal conditions on the magnitude and dynamics of the blood oxygenation level-dependent fMRI response. *J Cereb Blood Flow Metab* 2002; 22: 1042–1053.
25. Lindauer U, Leithner C, Kaasch H, et al. Neurovascular coupling in rat brain operates independent of hemoglobin

deoxygenation. *J Cereb Blood Flow Metab* 2010; 30: 757–768.
26. Rosengarten B, Dannhardt V, Burr O, et al. Neurovascular coupling in Parkinson's disease patients: effects of dementia and acetylcholinesterase inhibitor treatment. *J Alzheimers Dis* 2010; 22: 415–421.
27. Kisler K, Nelson AR, Montagne A, et al. Cerebral blood flow regulation and neurovascular dysfunction in Alzheimer disease. *Nat Rev Neurosci* 2017; 18: 419–434.
28. Rule RR, Schuff N, Miller RG, et al. Gray matter perfusion correlates with disease severity in ALS. *Neurology* 2010; 74: 821–827.
29. Murphy MJ, Grace GM, Tartaglia MC, et al. Widespread cerebral haemodynamics disturbances occur early in amyotrophic lateral sclerosis. *Amyotroph Lateral Scler* 2012; 13: 202–209.
30. Tamburrano G, Lala A, Locuratolo N, et al. Electroencephalography and visually evoked potentials during moderate hypoglycemia. *J Clin Endocrinol Metab* 1988; 66: 1301–1306.
31. Deutsch E, Sohmer H, Weidenfeld J, et al. Auditory nerve-brain stem evoked potentials and EEG during severe hypoglycemia. *Electroencephalogr Clin Neurophysiol* 1983; 55: 714–716.
32. Pries AR, Secomb TW, Gaehtgens P, et al. Blood flow in microvascular networks. Experiments and simulation. *Circ Res* 1990; 67: 826–834.
33. Alf MF, Duarte JMN, Schibli R, et al. Brain glucose transport and phosphorylation under acute Insulin-Induced hypoglycemia in mice: an ^{18}F-FDG PET study. *J Nucl Med* 2013; 54: 2153–2160.
34. Neil HA, Gale EA, Hamilton SJ, et al. Cerebral blood flow increases during insulin-induced hypoglycaemia in type 1 (insulin-dependent) diabetic patients and control subjects. *Diabetologia* 1987; 30: 305–309.
35. Tallroth G, Ryding E and Agardh CD. The influence of hypoglycaemia on regional cerebral blood flow and cerebral volume in type 1 (insulin-dependent) diabetes mellitus. *Diabetologia* 1993; 36: 530–535.
36. Wiegers EC, Becker KM, Rooijackers HM, et al. Cerebral blood flow response to hypoglycemia is altered in patients with type 1 diabetes and impaired awareness of hypoglycemia. *J Cereb Blood Flow Metab* 2017; 37: 1994–2001.
37. Sankar A, Khodai T, McNeilly AD, et al. Experimental models of impaired hypoglycaemia-associated counter-regulation. *Trends Endocrinol Metab* 2020; 31: 691–703.
38. Putzer G, Martini J, Spraider P, et al. Adrenaline improves regional cerebral blood flow, cerebral oxygenation and cerebral metabolism during CPR in a porcine cardiac arrest model using low-flow extracorporeal support. *Resuscitation* 2021; 168: 151–159.
39. Harder DR, Gebremedhin D, Narayanan J, et al. Formation and action of a P-450 4A metabolite of arachidonic acid in cat cerebral microvessels. *Am J Physiol* 1994; 266: H2098–H2107.
40. Metea MR and Newman EA. Glial cells dilate and constrict blood vessels: a mechanism of neurovascular coupling. *J Neurosci* 2006; 26: 2862–2870.
41. Kim KJ, Ramiro Diaz J, Iddings JA, et al. Vasculo-neuronal coupling: retrograde vascular communication to brain neurons. *J Neurosci* 2016; 36: 12624–12639.
42. Boynton GM, Engel SA, Glover GH, et al. Linear systems analysis of functional magnetic resonance imaging in human V1. *J Neurosci* 1996; 16: 4207–4221.
43. Polimeni JR and Lewis LD. Imaging faster neural dynamics with fast fMRI: a need for updated models of the hemodynamic response. *Prog Neurobiol* 2021; 207: 102174.
44. Seghouane A and Ferrari D. Robust hemodynamic response function estimation from fNIRS signals. *IEEE Trans Signal Process* 2019; 67: 1838–1848.